Pseudogap and anharmonic phonon behavior in $Ba_8Ga_{16}Ge_{30}$: An NMR study

Ali A. Sirusi[1,a)] and Joseph H. Ross, Jr.[1,2,b)]
[1]*Department of Physics and Astronomy, Texas A&M University, College Station, Texas 77843, USA*
[2]*Department of Materials Science and Engineering, Texas A&M University, College Station, Texas 77843, USA*

(Received 1 April 2016; accepted 18 July 2016; published online 1 August 2016)

We have performed ^{69}Ga, ^{71}Ga, and ^{137}Ba NMR on $Ba_8Ga_{16}Ge_{30}$, a clathrate semiconductor which has been of considerable interest due to its large figure of merit for thermoelectric applications. In measurements from 4 K to 450 K, we used measurements on the two Ga nuclei to separate the magnetic and electric quadrupole hyperfine contributions and thereby gain information about the metallic and phonon behavior. The results show the presence of a pseudogap in the Ga electronic states within the conduction band, superposed upon a large Ba contribution to the conduction band. Meanwhile the phonon contributions to the Ga relaxation rates are large and increase more rapidly with temperature than typical semiconductors. These results provide evidence for enhanced anharmonicity of the propagative phonon modes over a wide range, providing experimental evidence for enhanced phonon-phonon scattering as a mechanism for the reduced thermal conductivity. *Published by AIP Publishing.* [http://dx.doi.org/10.1063/1.4960054]

I. INTRODUCTION

Intermetallic clathrates have gained considerable attention in recent years due to their low thermal conductivities and thereby potential applications for high temperature thermoelectric devices.[1–3] Type-I $Ba_8Ga_{16}Ge_{30}$ has been intensively investigated as a result of its relatively high figure of merit $zT \approx 1$ among different type of clathrates.[2,4] The figure of merit is defined as $zT = S^2\sigma T/\kappa$, where S is the Seebeck coefficient, σ the electrical conductivity, κ the thermal conductivity, and T the temperature. Understanding the mechanism for low thermal conductivity is one of the major issues for these materials.

In this structure, the Ba atoms (called "guest" or sometimes "rattler") are encompassed in the cages constructed of Ga and Ge atoms. Although many studies have been done on type-I clathrates,[2] the underlying physics of low thermal conductivity and the roles of guest atoms in $Ba_8Ga_{16}Ge_{30}$ are still controversial. In one picture, the guest atom rattling can resonantly scatter phonons and make the thermal conductivity low.[5] In another scenario, it is the hybridization of the guest atom modes with the framework acoustic modes which results in an avoided crossing.[6] Moreover, recent studies using *ab initio* calculations[7] have connected the low thermal conductivity to nonresonant phonon scattering and a significant reduction of phonon relaxation times compared to the unfilled clathrates.

It has been shown that in type-I $Ba_8Ga_{16}Sn_{30}$[8,9] a low-temperature broad peak in the Ga NMR spin-relaxation rates exists corresponding to the off-center Ba rattling. Here we utilized the same procedure as Ref. 8 for the $Ba_8Ga_{16}Ge_{30}$ sample to separate the quadrupole and magnetic contributions to the relaxation rates. The results indicate rather different behavior with an enhanced contribution at high temperatures. In addition, Ba NMR shows a large contribution of Ba orbits to the conduction band.

II. EXPERIMENT

A. Synthesis and sample characterization

A polycrystalline $Ba_8Ga_{16}Ge_{30}$ sample was prepared from pure elements [Ge (pieces, 5N), Ga (ingot, 4N), and Ba (rod, 2N5)] with excess (4%) barium, and arc melted in an argon environment following by annealing in a BN crucible for one day at 950 °C and then three days at 700 °C in an evacuated sealed quartz tube. XRD measurements were performed on a Bruker D8 X-ray powder diffractometer. Rietveld refinement of the XRD data was performed using EXPGUI.[10,11] Fig. 1 shows the powder XRD and refinement. The sample is a type-I clathrate (space group $Pm\bar{3}n$ with a lattice constant $a = 10.7841$ Å) with a small amount of Ge impurity. Wavelength dispersive spectroscopy (WDS) measurements were carried out in a Cameca SX50 equipped with 4 wavelength-dispersive X-ray spectrometers on four points in the pulverized sample. The average results of WDS yielded $Ba_{7.89}Ga_{15.21}Ge_{30.79}$.

Hall coefficient and resistivity measurements were performed in a Quantum design Physical Property Measurement System. Based on the Hall results, a simple one-band model results in $n = 3.95 \times 10^{20}$ cm^{-3} at room temperature. If we apply the Zintl concept[12] (Ba^{2+}, Ga^{-1}) to the WDS results, we obtain $n = 4.5 \times 10^{20}$ cm^{-3} in good agreement with the Hall measurement result. The resistivity vs temperature (inset in Fig. 1) shows behavior characteristic of an n-type heavily doped semiconductor.

a)Electronic address: alisirusi@tamu.edu
b)Electronic address: jhross@tamu.edu

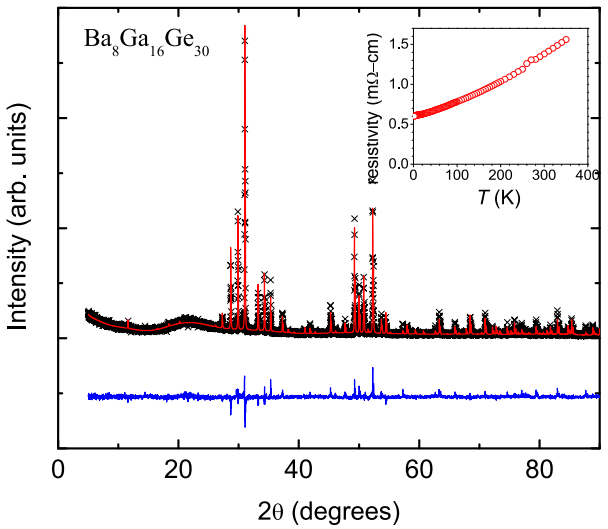

FIG. 1. Powder XRD spectrum at room temperature along with results of refinement and difference plots. Inset: resistivity vs T.

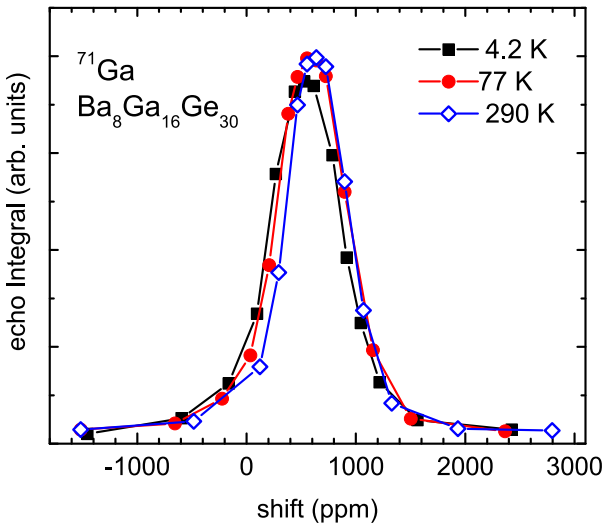

FIG. 2. ^{71}Ga spectra measured at 4.2 K, 77 K, and 290 K for the $Ba_8Ga_{16}Ge_{30}$ sample. Inset: the total magnetic shifts vs temperature.

For comparison of Ba contribution to the conduction band, we also have measured Ba NMR on a $Ba_8Ga_{16}Sn_{30}$ sample. The sample preparation method for the $Ba_8Ga_{16}Sn_{30}$ sample was reported in Ref. 8 and this sample was the same as measured in that reference.

B. NMR measurements

NMR experiments were carried out using a custom-built pulse spectrometer at a fixed field of 9 T. The ^{69,71}Ga and ^{137}Ba spectra were measured with respect to aqueous $Ga(NO_3)_3$ and $BaCl_2$, respectively. Measurements of Ga NMR utilized spin echo integration vs frequency, whereas the Ba NMR spectra were obtained by using CPMG sequences[13] where the echo integrals were achieved at each frequency by summing of consecutive echoes in the CPMG sequence.

NMR spin-lattice relaxation measurements (T_1) were obtained based on a magnetic relaxation mechanism using a stretched multi-exponential function for recovery of the central transition.[14] For spin 3/2, the central transition recovery function is $M(t)/M(0) = 1 - a(0.1e^{-(t/T_1)^\beta} + 0.9e^{-(6t/T_1)^\beta})$, where the exponent β is presumed to be due to a distribution of local environments. For measurements, the repetition rate was set greater than (5 times) T_1. Uncertainty in T_1 from the resulting fits is determined by statistical uncertainties, limited by the measurement signal-to-noise ratio. In the analysis, we used nuclear moment values (Q and γ) reported in Ref. 15. For magnetic shift contributions $\delta_{total} = \delta_{cs} + K$, we follow the convention $\delta_{cs} = (f - f_0)/f_0$ for chemical shifts, with f_0 the standard reference frequency and positive shifts having paramagnetic sign, while the Knight shifts (K) have an analogous definition.

III. RESULTS AND DISCUSSION

Figure 2 shows ^{71}Ga spectra of the $Ba_8Ga_{16}Ge_{30}$ sample obtained at 4.2 K, 77 K, and 290 K. Similar spectra (not shown) were obtained for ^{69}Ga. The line-shapes are superpositions of $m = 1/2$ to $-1/2$ transitions of three different Ga sites (6c, 16i, 24k).

The magnetic and quadrupole shift contributions were extracted from the line-shape centers of mass for each nucleus using $\Delta f/f_0 = \delta_{total} + BQ^2$, where δ_{total} is the magnetic shift, B is a constant, and Q is the nuclear quadrupole moment.

Table I shows the resulting magnetic shifts at different temperatures. The quadrupole shifts due to the second-order quadrupole mechanism give small negative shifts less than −3 kHz (−26 ppm) for ^{71}Ga, similar to the results for Cu NMR in the $Ba_8Cu_5Si_yGe_{41-y}$ samples.[16] For determining contributions in the magnetic shifts, we used the 4.2 K value of this shift to calculate the difference at other temperatures. The resulting magnetic shift δ_{total} can be further separated[14,17] into a Knight shift and chemical shift ($\delta_{total} = K + \delta_{cs}$), where here we identify δ_{cs} as the contribution due to orbital effects vs K which is due to conduction electron spins (and which will depend on sample doping). To separate this contribution, we utilized the relaxation times as described below.

As was mentioned above, the relaxation times were obtained by fitting the magnetization curve to a stretched multi-exponential function. The initial results for both ^{71}Ga and ^{69}Ga relaxation times showed that the β values for all temperatures could be fitted to 0.64 (within the range of

TABLE I. ^{71}Ga magnetic NMR shifts (δ_{total}), Knight shift (K), magnetic relaxation time (T_{1M}), and Korringa values at 4.2 K, 77 K, and 290 K for $Ba_8Ga_{16}Ge_{30}$ sample.

	4.2 K	77 K	290 K
δ_{total} (ppm)	597 ± 12	616 ± 12	665 ± 11
K (ppm)	305	326	375
T_{1M} (s)	7.12 ± 0.6	0.36 ± 0.02	0.070 ± 0.005
$K^2T_{1M}T$ (sK)	2.65×10^{-6}	2.94×10^{-6}	2.85×10^{-6}

±0.04). Therefore, we used the fixed $\beta = 0.64$ for all Ga relaxation recovery curve fittings.

The extracted spin-lattice relaxation rates ($1/T_1$) can be separated into magnetic $1/T_{1M}$ and quadrupole[8] terms $1/T_{1Q}$ by using the characteristic Q and γ dependencies: $1/^{69,71}T_1 = A\gamma^2_{69,71} + BQ^2_{69,71}$, where A and B are constants to be fitted at each temperature, while γ and Q are known constants. The phonon contribution (quadrupole mechanism) and carrier dominated term (magnetic) obey $1/T_{1Q} \propto Q^2$ and $1/T_{1M} \propto \gamma^2$, respectively, thus measurements for the two nuclei can be used to obtain the separated values with the uncertainties determined by those of the T_1 measurements. $1/T_{1M}$ and $1/T_{1Q}$ obtained from this procedure are shown in Fig. 3.

Note that in Ref. 18 the T_1 curves were fitted to a sum of multi-exponential curves attributed to crystallographic site occupancies of Ga. The resulting curves are similar to a stretched multi-exponential, and we find, for example, that our fitted T_1 is very close to the mean T_1 value obtained by fitting the data to a sum of two multi-exponential functions. However, we focus on the additional information obtained by separation of the magnetic and quadrupolar parts, as described below.

The magnetic relaxation rates can be fitted to a parabolic pseudogap[19,20] equation,

$$1/T_{1M} = aT + bT^3, \tag{1}$$

where $a = 0.0351 \pm 0.0030$ K^{-1} s^{-1} and $b = 1.70 \pm 0.25 \times 10^{-7}$ K^{-3} s^{-1} obtained from the fit. Eq. (1) can be derived by expanding the density of states, $g(E) = g_0 + g'(E - E_F) + \frac{1}{2}g''(E - E_F)^2$ in the vicinity of the Fermi energy (E_F) for the s-electrons,[21]

$$1/T_{1M} = \beta_S g_0^2 k_B T + \beta_S g_0 g'' \frac{\pi^2}{3}(k_B T)^3, \tag{2}$$

where $\beta_S = (64/9)\pi^3\hbar^3\gamma_e^2\gamma_n^2\langle|u_k^2(0)|\rangle^2_{E_F}$, and $\langle|u_k^2(0)|\rangle_{E_F}$ is the averaged square of the wave function at the nucleus over the Fermi surface. The magnetic relaxation rates thus fitted indicate a parabolic dependence of $g(E)$ around E_F with $g_0 = 0.0087 \pm 0.0007$ 1/(eV atom) and $g''/g_0 = 198 \pm 29$ eV^{-2} (note that we used the Ga Fermi-contact hyperfine field[14] 6.2 MG).

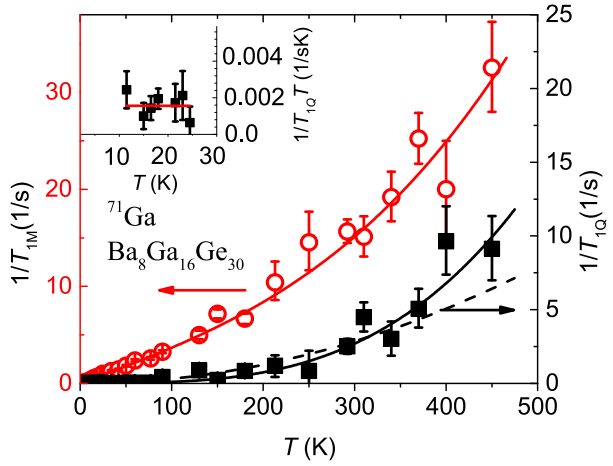

FIG. 3. $1/T_{1M}$ (magnetic spin-lattice relaxation contributions) and $1/T_{1Q}$ (quadrupole mechanism) as a function of temperature. The lines are fitted curves as explained in the text. The dashed line is the T^2 fit. The inset shows $1/TT_{1Q}$ below 30 K.

The Knight shifts also can be expressed as[21]

$$K = K_0\Big(1 + \frac{\pi^2}{6}(k_B T)^2\Big[\frac{g''}{g_0} - \Big(\frac{g'}{g_0}\Big)^2\Big]\Big), \tag{3}$$

where $K_0 = (4/3)\pi\hbar^2\gamma_e\langle|u_k^2(0)|\rangle_{E_F} g_0$. Note that Eq. (3) contains a term which depends on g', whereas Eq. (2) is independent of g'. Furthermore, only when $g' = 0$ is the product $K^2T_{1M}T$ generated from these two expressions temperature-independent, reducing to the usual Korringa product,[13,14] which is $K^2T_{1M}T = 2.8 \times 10^{-6}$ sK for ^{71}Ga. To test for this condition, we first assumed the Korringa product to have this value and obtained the chemical shift ($\delta_{cs} = \delta_{total} - K$) using the resulting K along with the experimental δ_{total}. This procedure yielded nearly T-independent values of δ_{cs} as expected (variation of 3%), an indication that indeed $g' = 0$ is a good model in this case, with the temperature dependence coming from the g'' term. Finally we replaced δ_{cs} by the mean value obtained this way, $\delta_{cs} = 290$ ppm, yielding values for K and $K^2T_{1M}T$ given in Table I. The chemical shift thus extracted in very close to that[8] of $Ba_8Ga_{16}Sn_{30}$ (Table II).

Extraction of the Knight shifts from the T_1 is model-dependent, relying on the Korringa relation as noted above. However this relation is expected to be reliable for semiconductors doped well into the metallic regime as in the present case, and the consistency of the Korringa-derived results vs temperature give additional confidence in this result. Thus we believe that the uncertainty in K is dominated by the known uncertainty in T_1, thus resulting in the approximately 10% variation of the calculated Korringa products in Table I. From the positive T^3 coefficient b (Eq. (1)), we thereby determine that E_F is at a minimum point in $g(E)$, corresponding to a pseudogap configuration. As a characterization of the shape of this pseudogap, the fitted parabolic rise in $g(E)$ would reach $2g_0$ at energies corresponding to a width of 0.2 eV.

Note that an increase in T_1^{-1} vs temperature comparable to our ^{71}Ga results was reported for ^{71}Ga NMR in a similarly doped $n = 2 \times 10^{20}$ cm^{-3} sample.[18] This behavior thus appears to be a general feature of $Ba_8Ga_{16}Ge_{30}$ materials with these doping levels. On the other hand, in a sample Ref. 22 with $n = 8.7 \times 10^{19}$ cm^{-3}, $1/T_{1M}$ instead was observed to increase with decreasing temperature, with temperature dependence comparable to what has been reported for GaAs at doping

TABLE II. Lattice constants (a), Ga NMR chemical shifts ($^{Ga}\delta_{cs}$), ^{137}Ba T_1 (for 77 K at the peak positions), and total Ba shift ($^{Ba}\delta_{total}$) for $Ba_8Cu_5Ge_{41}$ obtained from two-site quadrupole fit,[16] and $Ba_8Ga_{16}Ge_{30}$, and $Ba_8Ga_{16}Sn_{30}$[8] samples obtained by fitting to single Gaussians.

Compounds	a (Å)	$^{Ga}\delta_{cs}$ (ppm)	^{137}BaT_1 (ms)	$^{Ba}\delta_{total}$ (ppm)
$Ba_8Cu_5Ge_{41}$	10.692	...	1042	1390
$Ba_8Ga_{16}Ge_{30}$	10.784	290	140	1690
$Ba_8Ga_{16}Sn_{30}$	11.585	300	3220	515

levels just below the metal-insulator transition.[23] Thus we assume the mobility edge is close to this value based on the similarity to what is observed in GaAs; however, for the present sample, the Korringa behavior indicates more standard metallic behavior.

Turning to the quadrupole contribution, $1/T_{1Q}$, also plotted in Fig. 3, we see that there is no low-temperature peak in relaxation rate, such as observed in the rattler system $Ba_8Ga_{16}Sn_{30}$, which exhibits a broad peak[8,9] near 10 K. Since atomic vibrations are coupled most strongly to the nuclei through the electric quadrupole hyperfine fields, the separated $1/T_{1Q}$ contribution provides a particularly sensitive test for such oscillations. As seen in the inset of Fig. 3, $1/T_{1Q}T$ does remain unexpectedly nonzero at the lowest observed temperatures, however the values are quite small, and the results approach a constant rather than exhibiting a rattler peak.

In contrast to the lack of a low-temperature rattler peak, at high temperatures $1/T_{1Q}$ rises quite rapidly, a result which may signify strong anharmonicity for the propagating phonons, as shown below. In order to characterize the behavior, we fitted $1/T_{1Q}$ to a function T^n, giving the curve shown in Fig. 3. This fitting gives $1/T_{1Q} \propto T^{3.2\pm0.3}$. This temperature dependency does not follow the usual power law as expected in a Debye model,[24]

$$\frac{1}{T_{1Q}} \propto Q^2\left(\frac{T}{\Theta_D}\right)^7 \int_0^{\Theta_D/T} \frac{e^x x^6}{(e^x-1)^2} dx, \qquad (4)$$

where Θ_D is the Debye temperature. Eq. (4) approaches a T^2 limit (see the dashed line in Fig. 3). However it has been shown[24,25] that with the presence of anharmonic terms, the usual 2-phonon relaxation process becomes superseded at high temperatures by a multi-phonon term with $1/T_{1Q}$ proportional to T^3 or T^4. In semiconductors, T^2 behavior is typically observed over a wide temperature range, for example, Ref. 26 through 1000 K in InAs. Thus the fitted $1/T_{1Q} \propto T^{3.2}$ is anomalous, and we assign this result to a crossover to an enhanced high-temperature anharmonic term. In addition, the magnitude of the high-temperature $1/T_{1Q}$ is large compared to other semiconductors, which helps to confirm the presence of an additional quadrupole relaxation mechanism.

To compare amplitudes of the phonon-induced relaxation rate, it is useful to consider NMR as reported in other Ga-containing semiconductors, since the parameters specific to the Ga ion will be the same. To do this, we replaced the magnetic multi-exponential with a stretched single-exponential, essentially giving the mean T_1 for comparison. The result, for example, in the ^{71}Ga case at 300 K, is $1/T_{1Q} = 13$ s^{-1}, which can be compared to reported ^{71}Ga rates in GaAs,[27] GaSb,[27] and GaN[28] of $1/T_{1Q} = 3$, 2.5, and 1 s^{-1}, respectively. The enhanced rate in $Ba_8Ga_{16}Ge_{30}$ is consistent with a larger phase space for phonon-based relaxation processes, as would also be expected given the case that the additional anharmonic mechanism becomes important in this material.

A ^{137}Ba NMR spectrum for the $Ba_8Ga_{16}Ge_{30}$ sample at 77 K is shown in Fig. 4 by the solid triangles. This spectrum is a superposition of two types of Ba cage (sites 2*a* and 6*d*). To compare this line-shape, we also measured the 4 K ^{137}Ba

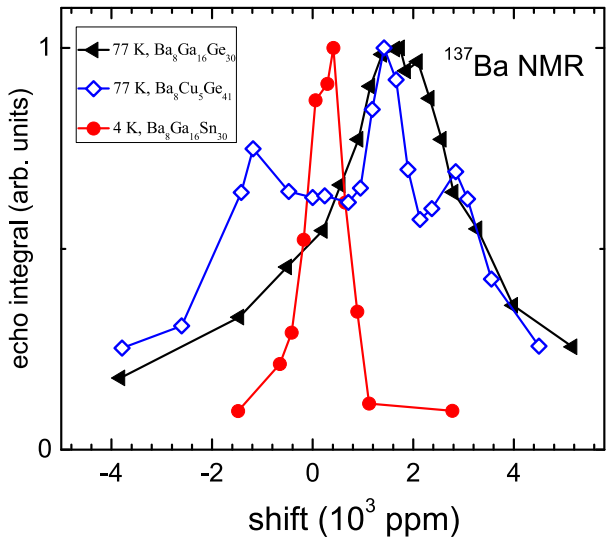

FIG. 4. ^{137}Ba NMR spectrum measured at 77 K for $Ba_8Ga_{16}Ge_{30}$, along with that of $Ba_8Ga_{16}Sn_{30}$ at 4 K, and the previously reported[16] results for $Ba_8Cu_5Ge_{41}$ at 77 K.

spectrum of $Ba_8Ga_{16}Sn_{30}$ (filled circles; sample characteristics reported in Ref. 8) and also display the previously reported ^{137}Ba spectrum of a $Ba_8Cu_5Ge_{41}$ sample (open diamonds; Ref. 16). The smaller shift and narrow Ba resonance for $Ba_8Ga_{16}Sn_{30}$ corresponds to its larger lattice constant,[29] clearly showing the weak interaction of Ba with the framework atoms, and thereby the smaller quadrupole broadening. $Ba_8Cu_5Ge_{41}$ has small cages and an ordered arrangement of Cu atoms[16] and exhibits a superposition of two well-defined spectra for the two cages, including a large quadrupole broadening for the 6*d* site. By contrast, the lack of structure for the case of $Ba_8Ga_{16}Ge_{30}$ presumably reflects a superposition of many arrangements of Ga ion neighbors, while the large shift reflects a significant participation of Ba in the conduction band, as shown below.

The ^{137}Ba relaxation times sampled at the center of each resonance at 77 K are given in Table II. The T_1 is the largest for $Ba_8Ga_{16}Sn_{30}$, and while we have not assessed the size of the rattling-type quadrupole contribution[8] in the Ba NMR, clearly the carrier-related Korringa contribution for this sample is small. By contrast the much shorter T_1 for $Ba_8Ga_{16}Ge_{30}$ indicates a much larger Korringa contribution. This is made clear by noting that typical Ba chemical shifts[30] are between 100 and 500 ppm which means the large shift for $Ba_8Ga_{16}Ge_{30}$ must be largely due to carriers (Knight shift). In addition, relative to the measured $1/T_1$ for $Ba_8Ga_{16}Ge_{30}$, the 77 K quadrupole contribution to T_1^{-1} is expected to be very small (compare Fig. 3), so we also assume that the observed T_1 is entirely magnetic in origin. Using the known Korringa product $K^2T_1T = 21 \times 10^{-6}$ sK for the ^{137}Ba nucleus, we obtain $K = 1400$ ppm, so that the remainder of the observed shift, 460 ppm, can be assigned as a chemical shift. Since as noted above, the expected Ba chemical shift range ends at 500 ppm,[30] this result seems quite reasonable. Note also that metallic shifts due to Ba *p* and *d* orbitals are negative,[14] and with considerably smaller hyperfine fields, thus if such contributions were to dominate, the results would imply an

unphysically large chemical shift. Thus it appears that the metallic part of the shift must be an ordinary Knight shift of positive sign.

The Korringa T_1^{-1} (and corresponding Knight shift) identified above can also be used to obtain the Ba *s*-electron contribution to the local density of states, using the Ba hyperfine field[31] $H_s^{HF} = 3.6$ MG. Since[14] $K = H_s^{HF}\mu_B g_s(E_F)$ for metals, we obtain $g_s(E_F) = 0.067$ (eV atom)$^{-1}$. Note that this result depends on the measured T_1, as well as the Ba hyperfine field value. It has been established[14] that this method works well for simple metals in predicting the Korringa values (with 10% or 20% certainty), and as shown above the results bring the extracted chemical shift into the expected range. Thus even allowing for a small quadrupole T_1 contribution, these results point to a very large Ba *s*-contribution. Compared to $g_0(E_F) = 0.0087$ (eV atom)$^{-1}$ at the bottom of the pseudogap, obtained for the Ga sites as noted above, the *s*-contribution for Ba is 7.7 times larger, implying a very large fractional contribution due to Ba *s*-states in the conduction band.

Previous electronic structure calculations[32] for $Ba_8Ga_{16}Ge_{30}$ have indicated a large Ba contribution to the conduction band density of states, including[33] a Ba *d*-dominated peak in a relatively narrow energy region. A recent result[34] also indicates that Ba *s*-states play a significant role in the region just above the gap. The present results confirm a large Ba contribution, and we show that the framework contribution (at least that of Ga atoms) is in fact considerably smaller than that of the Ba states. A large Ba $g(E_F)$ peak, combined with the pseudogap observed in the framework states, has the characteristics typically associated with *s-d* hybridization gap behavior,[35] which may further depress the framework contribution in this case. The observed pseudogap must have a significant effect on the thermoelectric properties.

Returning to the enhanced phonon contribution to the Ga quadrupole T_1, the mechanism[25] relies on enhanced anharmonicity of the propagative phonon modes, throughout *k*-space rather than a single localized mode, with no dependence on phonon velocity. Recently several reports have focused on the contributions of these effects toward lowering the thermal conductivities. In silicon clathrates,[36] model calculations have shown that the clathrate structure itself tends to induce enhanced anharmonicity as well as lowered propagation velocity, while in $Ba_8Ga_{16}Ge_{30}$,[7] it has been proposed that presence of the Ba filler atoms strongly enhances the anharmonic contribution. A previous neutron scattering study[6] of $Ba_8Ga_{16}Ge_{30}$ focused on the anti-crossing of phonon levels near the frequency of the Ba vibrational mode, and showed that scattering by this mode alone could not account for the reduced thermal conductivity. On the other hand, a recent inelastic neutron study[37] of $Ba_8Ge_{40+x}Ni_{6-x}$ indicated a further hybridization of Ba-centered vibrational modes with propagative modes across a wide range of phonon energies, leading to a filtering effect which may contribute to the low thermal conductivity. This is similar to recent findings for a Si clathrate[38] based on computational and inelastic x-ray studies. By contrast, the NMR process[24,25] leading to an enhanced phonon-contributed T_1^{-1} relies upon a multi-phonon mechanism which depends specifically upon an inelastic phonon-phonon interaction. It is not clear from this how large is the contribution to the reduced thermal conductivity; however, the present results indicate an enhancement of such anharmonic processes relative to the behavior of ordinary semiconductors. The NMR results provide experimental evidence for such an anharmonic contribution, while the contrast with the behavior of $Ba_8Ga_{16}Sn_{30}$[8] illustrates directly the different contributions of localized vs propagating phonon modes in these materials.

IV. CONCLUSIONS

We measured ^{69}Ga, ^{71}Ga, and ^{137}Ba on $Ba_8Ga_{16}Ge_{30}$ from 4 K to 450 K. The metallic shifts and spin-lattice relaxation results show the presence of a pseudogap in Ga states within the conduction band, superposed upon a large Ba *s*-electron contribution to the conduction band density of states compared to other type-I clathrates. Meanwhile, the quadrupole contributions to the Ga relaxation rates are large and increasing more rapidly with temperature than in typical semiconductors. These results provide evidence for enhanced anharmonicity of the propagative phonon modes, a result with considerable importance for the reduction of thermal conductivity for thermoelectric applications.

ACKNOWLEDGMENTS

This work was supported by the Robert A. Welch Foundation (Grant No. A-1526).

[1]J. Martin, H. Wang, and G. S. Nolas, Appl. Phys. Lett. **92**, 222110 (2008).
[2]T. Takabatake, K. Suekuni, T. Nakayama, and E. Kaneshita, Rev. Mod. Phys. **86**, 669 (2014).
[3]*The Physics and Chemistry of Inorganic Clathrates*, edited by G. S. Nolas (Springer, Netherlands, 2014).
[4]A. Saramat, G. Svensson, A. E. C. Palmqvist, C. Stiewe, E. Mueller, D. Platzek, S. G. K. Williams, D. M. Rowe, J. D. Bryan, and G. D. Stucky, J. Appl. Phys. **99**, 023708 (2006).
[5]J. L. Cohn, G. S. Nolas, V. Fessatidis, T. H. Metcalf, and G. A. Slack, Phys. Rev. Lett. **82**, 779 (1999).
[6]M. Christensen, A. B. Abrahamsen, N. B. Christensen, F. Juranyi, N. H. Andersen, K. Lefmann, J. Andreasson, C. R. H. Bahl, and B. B. Iversen, Nat. Mater. **7**, 811 (2008).
[7]T. Tadano, Y. Gohda, and S. Tsuneyuki, Phys. Rev. Lett. **114**, 095501 (2015).
[8]X. Zheng, S. Y. Rodriguez, and J. H. Ross, Jr., Phys. Rev. B **84**, 024303 (2011).
[9]H. Tou, K. Sonoda, K. Furumoto, H. Kotegawa, K. Suekuni, M. A. Avila, and T. Takabatake, J. Phys. Soc. Jpn. **82**, 114603 (2013).
[10]B. H. Toby, J. Appl. Crystallogr. **34**, 210 (2001).
[11]A. C. Larson and R. B. V. Dreele, Los Alamos National Laboratory Report No. LAUR 86–748, 1994.
[12]E. Zintl, Angew. Chem. **52**, 1 (1939).
[13]C. P. Slichter, *Principles of Magnetic Resonance* (Springer-Verlag GmbH, 1996).
[14]G. Carter, L. Bennett, and D. Kahan, Prog. Mater. Sci. **20**, 1 (1976).
[15]R. K. Harris and E. D. Becker, J. Magn. Reson. **156**, 323 (2002).
[16]A. A. Sirusi, J. H. Ross, Jr., X. Yan, and S. Paschen, Phys. Chem. Chem. Phys. **17**, 16991 (2015).
[17]*Calculation of NMR and EPR Parameters: Theory and Applications*, 1st ed., edited by M. Kaupp, M. Bühl, and V. G. Malkin (Wiley-VCH, 2004).
[18]D. Arčon, A. Zorko, P. Jeglič, J. Xu, J. Tang, Y. Tanabe, S. Heguri, and K. Tanigaki, J. Phys. Soc. Jpn. **82**, 014703 (2013).
[19]J. Dolinšek, M. Klanjšek, T. Apih, A. Smontara, J. C. Lasjaunias, J. M. Dubois, and S. J. Poon, Phys. Rev. B **62**, 8862 (2000).

[20]X.-P. Tang, E. A. Hill, S. K. Wonnell, S. J. Poon, and Y. Wu, Phys. Rev. Lett. **79**, 1070 (1997).
[21]J. Winter, *Magnetic Resonance in Metals* (Clarendon Press, Oxford, 1971).
[22]X. Zheng, Ph.D. thesis, Texas A&M University, 2012.
[23]D. Kölbl, D. M. Zumbühl, A. Fuhrer, G. Salis, and S. F. Alvarado, Phys. Rev. Lett. **109**, 086601 (2012).
[24]A. Abragam, *The Principles of Nuclear Magnetism* (Oxford Science Publications, 1961).
[25]R. C. Zamar and C. E. González, Phys. Rev. B **51**, 932 (1995).
[26]B. Tasche and H. Richtering, Phys. Status Solidi A **95**, 565 (1986).
[27]J. A. McNeil and W. G. Clark, Phys. Rev. B **13**, 4705 (1976).
[28]M. Corti, A. Gabetta, M. Fanciulli, A. Svane, and N. E. Christensen, Phys. Rev. B **67**, 064416 (2003).
[29]G. Nolas, J. L. Cohn, J. S. Dyck, C. Uher, G. A. Lamberton, and T. M. Tritt, J. Mater. Res. **19**, 3556 (2004).
[30]I. L. Moudrakovski, *Annual Reports on NMR Spectroscopy* (Elsevier B.V., 2013), pp. 129–240.
[31]R. E. Watson and L. H. Bennett, Phys. Rev. B **15**, 502 (1977).
[32]C. Gatti, L. Bertini, N. P. Blake, and B. B. Iversen, Chem. - Eur. J. **9**, 4556 (2003).
[33]G. K. H. Madsen, K. Schwarz, P. Blaha, and D. J. Singh, Phys. Rev. B **68**, 125212 (2003).
[34]D. Li, L. Fang, S. Deng, H. Ruan, M. Saleem, W. Wei, and C. Kong, J. Electron. Mater. **40**, 1298 (2011).
[35]G. T. de Laissardiere, D. Nguyen-Manh, and D. Mayou, Prog. Mater. Sci. **50**, 679 (2005).
[36]G. K. H. Madsen, A. Katre, and C. Bera, Phys. Status Solidi A **213**, 802 (2016).
[37]H. Euchner, S. Pailhès, L. T. K. Nguyen, W. Assmus, F. Ritter, A. Haghighirad, Y. Grin, S. Paschen, and M. de Boissieu, Phys. Rev. B **86**, 224303 (2012).
[38]S. Pailhès, H. Euchner, V. M. Giordano, R. Debord, A. Assy, S. Gomès, A. Bosak, D. Machon, S. Paschen, and M. de Boissieu, Phys. Rev. Lett. **113**, 025506 (2014).